

# Repetition rate increase and diffraction-limited focal spots for a nonthermal-equilibrium 100-TW Nd:glass laser chain by use of adaptive optics

B. Wattellier,\* J. Fuchs,<sup>†</sup> J. P. Zou, K. Abdeli, and H. Pépin

*Laboratoire pour l'Utilisation des Lasers Intenses, Unité Mixte de Recherche 7605, Centre Nationale de la Recherche Scientifique, École Polytechnique, Commissariat à l'Énergie Atomique, and Université Paris VI, École Polytechnique, 91128 Palaiseau Cedex, France*

C. Haefner

*Gesellschaft für Schwerionenforschung mbH, 64291 Darmstadt, Germany*

Received June 28, 2004

Dynamic wave-front correction is applied before each shot on a 100-TW, 30-J/300-fs high-power laser facility by use of an adaptive-optics system. This system allows us to increase the repetition rate of high-energy lasers while maintaining excellent and constant beam focusability with a Strehl ratio of  $>0.75$  despite the amplifiers' not being in thermal equilibrium. The best results in terms of the highest Strehl ratio and intensities are obtained when locking the system on wave-front sensing after pulse recompression. © 2004 Optical Society of America

OCIS codes: 140.7090, 140.3530, 120.5060.

Ultraintense lasers using the chirped-pulse amplification (CPA) technique<sup>1</sup> are currently mainly limited in terms of achievable repetition rate and focusability. Indeed spectral distortion can nowadays be precompensated for by spectral shaping<sup>2</sup> to produce a compressed pulse that is as short as possible. Also, higher levels of recompressed energy are now available by use of higher-damage-threshold dielectric-coated diffraction gratings. Enhancement in the repetition rate and focusability for an optimal use of the delivered power is limited by thermal load in the amplifiers. Thermal load in high-repetition-rate systems can be efficiently handled by cooling the Ti:sapphire amplifiers.<sup>3</sup> However, for glass systems with a lower repetition rate, even for a single shot, thermal load induces wave-front distortions. If one tries to increase the repetition rate above the dissipation time of the thermal load, cumulative thermal load appears and the focusability worsens. This is why most flash-lamp-pumped high-energy laser chains, with long thermalization time, have a low repetition rate. In this Letter we show for the first time to our knowledge that, by use of an adaptive-optics (AO) system<sup>4–6</sup> that dynamically corrects the laser wave front for each shot, we are able to increase the repetition rate of a high-energy 100-TW laser while maintaining excellent and reproducible focusability on every shot.

In the Laboratoire pour l'Utilisation des Lasers Intenses (LULI) 100-TW facility,<sup>7</sup> stretched pulses are preamplified in a Ti:sapphire linear regenerative amplifier up to 1 mJ; then they seed single-pass mixed-glass Nd:glass rods and disk amplifiers (see Fig. 1) with a final beam diameter of 90 mm. To abate propagation effects that cause intensity modulations, low-pass spatial filtering and relay imaging between the amplifiers is applied. Only after the disk amplifier does the beam freely propagate to and through the compressor and toward the target chamber. The chain delivers recompressed pulses (in vacuum) of  $\sim 30$  J in  $\sim 300$  fs (as measured by second-order auto-

correlation) at a  $\lambda = 1057$  nm central wavelength, resulting in laser power as high as 100 TW.

The repetition rate is imposed by the relaxation time of the thermal load in the amplifiers. Monitoring the evolution of wave-front distortions after a full-energy shot, as shown in Fig. 2(a), we find that the time it takes to reduce distortions to levels observed previous to a shot is 40 min. As a probe, we use the 1 mJ/10 Hz beam from the regenerative Ti:sapphire preamplifier that propagates through the whole chain. Using the CPA system at a higher repetition rate induces a rapid degradation of the laser beam intrinsic focusability, as illustrated in Figs. 2(b) and 2(c). In this case note that no wave-front corrector is implemented in the laser chain. After five full-energy shots every 20 min, the central peak of the focal spot becomes strongly asymmetric [see Fig. 2(c)]. The wave front becomes predominately aberrated by thermal lens effects and thermal birefringence astigmatism. Static compensation of the aberrations could not maintain the focusability since the aberrations are cumulative.

Dynamic wave-front correction is provided by an AO system that includes a 100-mm-diameter dielectric-coated deformable mirror (DM). The DM is positioned before compression as the reflector at the end of the double-pass disk amplifier (see Fig. 1). It is coupled to wave-front measurements (see Fig. 1) to lock the wave front toward a reference (usually flat). The DM has a high damage threshold that allows correction after the last amplifier, avoiding issues associated with aberration precompensation.<sup>5</sup> The home-designed convergence loop is described in detail in Ref. 9. The electrode pattern of the DM allows 30 independent wave-front correction channels for low-order aberration correction with strokes of  $\pm 5$   $\mu\text{m}$ . To have an optimum correction capability, we apodized the laser beam to a diameter 20% smaller than the mirror aperture.<sup>9</sup>

As shown in Fig. 1, to evaluate the importance of wave-front degradation induced by the large optics

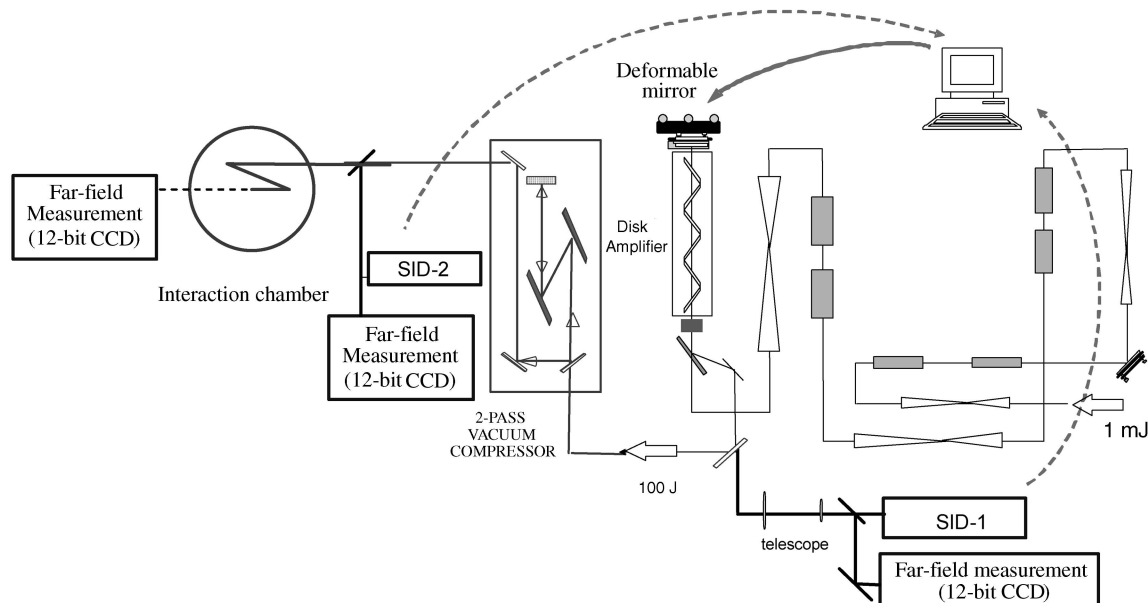


Fig. 1. Layout of the LULI 100-TW facility amplifiers and of the implementation of the AO system. SID-1 and SID-2 are the two achromatic three-wave lateral shearing interferometers<sup>8</sup> used as wave-front sensors.

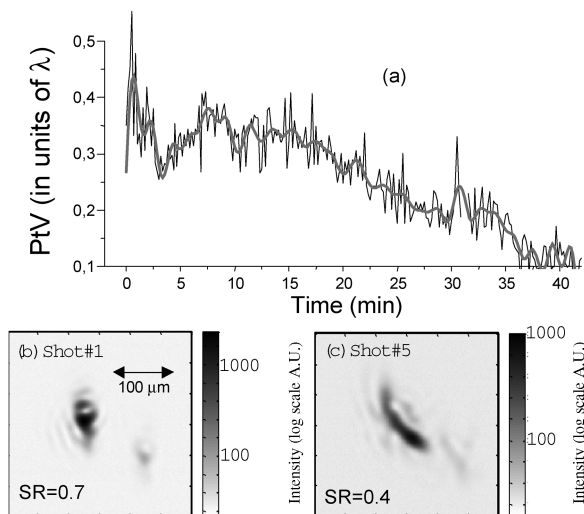


Fig. 2. (a) Time evolution of the peak to valley (PtV) of the wave front after a full-energy shot as recorded by SID-1. (b), (c) Measured focal spot after pulse compression for the first and fifth shots of five full-energy shots every 20 min and without wave-front correction. The focusing is done by an  $f = 1200$  mm diffraction-limited lens positioned after a leak through a mirror to test the intrinsic focusability. The spot at the lower right is due to reflection. Strehl ratios (SR) are as indicated.

inside the compressor, such as diffraction gratings, the closed-loop is performed either with a wave-front sensor placed before the compressor (SID-1) or with one placed after (SID-2). To optimize the wave-front correction, the DM should ideally be imaged on the wave-front sensor's entrance pupil. This is the case for SID-1. Since there is no image relay after the last disk amplifier, it was not possible to image the DM plane on SID-2; it images a plane between the two gratings inside the compressor. For each sensor, before each shot, by use of the low-energy 10-Hz beam of the regenerative amplifier that propagates through

the whole optical chain, the loop is made to converge toward the recorded flat reference wave front. Convergence is typically achieved in two or three iterations at 10 Hz. Phase correction is performed several seconds before each shot to avoid deviation of the phase.

To test the effectiveness of the AO loop in improving the laser's repetition rate while keeping a good focusability, we carried out a sequence of full-energy shots every 20 min, so that the laser was away from thermal equilibrium.

When correction is performed with SID-1, the phase in the sensor's plane is repeatedly flattened to the fluctuation level, i.e.,  $0.15\lambda$  PtV and  $0.03\lambda$  rms typically. Also, the focal spots recorded in the same plane are nearly diffraction limited and reproducible over the series of five shots with a Strehl ratio of  $>0.9$ , as shown in Figs. 3(a) and 3(b). This is expected since the plane of observation is equivalent to the one in which the phase maps are observed to be nearly flat. The focusability degradation from shot to shot illustrated in Fig. 2 is thus canceled out by dynamic correction of the wave front before each shot every 20 min: The laser chain can be used at a higher repetition rate than the one imposed by the amplifiers' cooling time. However, the compression and focusing optics degrade the excellent focusability observed before compression: One observes after compression a lower intrinsic (i.e., measured with a long focal lens) focusability than what is measured before compression [see Fig. 4(d)], because of the aberrations in the compressor and the target area.

Performing wave-front correction with SID-2 allows us to obtain both an improved repetition rate and an excellent intrinsic focusability. This is achieved by first performing a convergence with SID-1. Then, when the level of aberrations as seen after compression is already low, we switch to locking the loop on SID-2. The wave-front PtV is reduced compared with when the correction is performed before compression from  $1\lambda$  to  $0.3\lambda$  [see Fig. 4(a)]. The Strehl ratio of the

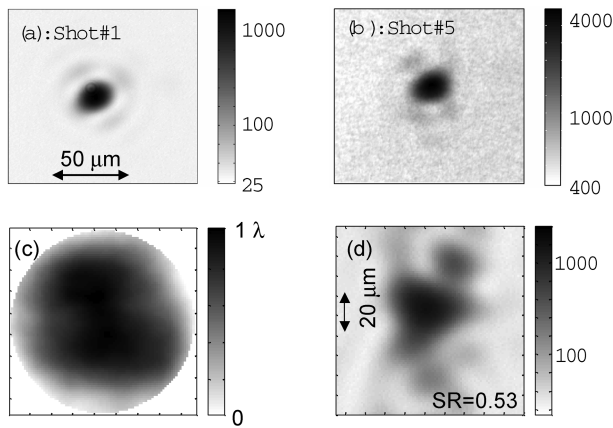


Fig. 3. (a), (b) Measured focal spot (with a lens) before pulse compression for the first and fifth shots of five full-energy shots every 20 min and with wave-front correction locked on SID-1. (c) Phase map and (d) focal spot (with a lens) measured after compression for the same shot as (b). Gray scales for the focal spot images are in logarithmic scale.

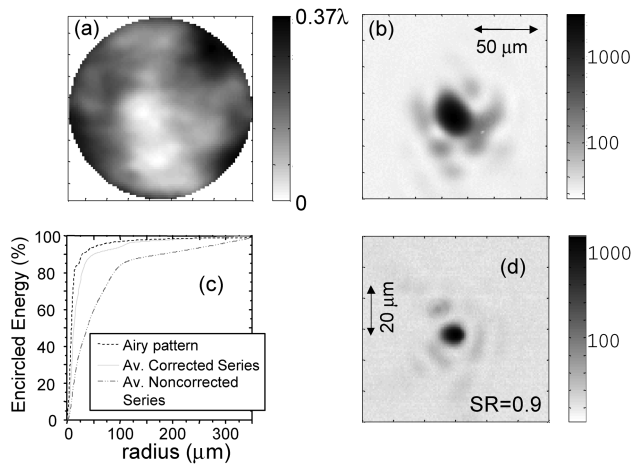


Fig. 4. (a) Phase map and (b) focal spot measured (with a lens) after compression for the fifth shot of five full-energy shots every 20 min and with wave-front correction locked on SID-2. (c) Encircled energy for a perfect Airy spot, for the average spot with wave-front correction [i.e., the spot in (b)], and for the average spot without wave-front correction (i.e., the spot in Fig. 2). (d) Same as (b), but the focusing is done with an  $f/4.5$  off-axis parabola. Gray scales for the focal spot images are in logarithmic scale.

focal spot evolves around 0.75 and can reach 0.9 [see Fig. 4(b)], still depending on the residual wave-front fluctuations after correction. This variation, higher than when locking on SID-1, may originate from the lesser stability of the loop that uses SID-2. The result of this convergence is to compare with Fig. 3(d) when correction was provided by SID-1 (Strehl ratio of 0.5) and with Fig. 2 without correction (Strehl ratio of 0.25 after five shots). This represents an improvement of a factor  $>3$  in the peak intensity. If we average the encircled energy curves [see Fig. 4(c)], we find that for noncorrected shots less than 30% of the energy was contained in the central disk. With dynamic wave-front correction this grows to more than 70%, and the focusing pattern in the far field can be

reproduced reliably for each shot. Under the same conditions, at full energy, we tested the focusability in more realistic conditions for experiments, i.e., using an off-axis parabola. This also yields an excellent focus, as shown in Fig. 4(d). The FWHM of the focal spot is  $4.9 \mu\text{m}$ , and the peak intensity is  $>1.5 \times 10^{20} \text{ W cm}^{-2}$ . With this correction an  $f/1$  off-axis parabola would yield a peak intensity as high as  $3.4 \times 10^{21} \text{ W cm}^{-2}$ .

In conclusion, using an adaptive-optics system on a 100-TW CPA laser system has allowed us to increase the repetition rate by a factor 2 while obtaining excellent (Strehl ratio of  $>0.75$ ) and reproducible focusing, although the laser chain is under the influence of cumulative thermal effects. This represents a significant enhancement of the performance of a high-power laser facility such as the one used for this study. The reduction of the repetition rate in the present study is limited by the induced birefringence in the amplifiers. Since the laser chain outputs 100 J, it is foreseeable to further increase the repetition rate by increasing the birefringence while still having 40 J in  $p$  polarization (which is the present acceptable limit for the compressor) in the output of the amplifiers.

We acknowledge the expert support of C. LeBras and C. Félix of the LULI laser team. This work was supported by grant E1127 from Région Ile-de-France, European Adaptool Research and Technological Development contract HPRI-CT-1999-50012, corporate support from General Atomics, and University of Nevada, Reno, grant DE-FC08-01NV14050. J. Fuchs's e-mail address is fuchs@physics.unr.edu.

\*Present address, Phasics, Campus de l'École Polytechnique, Bâtiment 404, 91128 Palaiseau, France.

†Present address, Department of Physics, MS-220, University of Nevada, Reno, Nevada 89557.

## References

1. D. Strickland and G. Mourou, *Opt. Commun.* **56**, 219 (1985).
2. F. Verluise, V. Laude, Z. Cheng, Ch. Spielmann, and P. Tournais, *Opt. Lett.* **25**, 575 (2000).
3. M. Pittman, S. Ferré, J. P. Rousseau, L. Notebaert, J. P. Chambaret, and G. Chériaux, *Appl. Phys. B* **74**, 529 (2002).
4. F. Druon, G. Chériaux, J. Faure, J. Nees, M. Nantel, A. Maksimchuk, G. Mourou, J.-C. Chanteloup, and G. Vdovin, *Opt. Lett.* **23**, 1043 (1998).
5. D. M. Pennington, C. G. Brown, T. E. Cowan, S. P. Hatchett, E. Henry, S. Herman, M. Kartz, M. Key, J. Koch, A. J. MacKinnon, M. D. Perry, T. W. Phillips, M. Roth, T. C. Sangster, M. Singh, R. A. Snavely, M. Stoyer, B. C. Stuart, and S. C. Wilks, *IEEE J. Sel. Top. Quantum Electron.* **6**, 676 (2000).
6. H. Baumhacker, G. Pretzler, K. J. Witte, M. Hegelich, M. Kaluza, S. Karsch, A. Kudryashov, V. Samarkin, and A. Roukossouev, *Opt. Lett.* **27**, 1570 (2002).
7. J. P. Zou, J. Fuchs, B. Wattellier, J. C. Chanteloup, and C. Haefner, *Proc. SPIE* **5137**, 188 (2003).
8. J. Primot and L. Sogno, *J. Opt. Soc. Am. A* **12**, 2679 (1995).
9. B. Wattellier, J. Fuchs, J. P. Zou, J. C. Chanteloup, H. Bandulet, P. Michel, C. Labaune, S. Depierreux, A. Kudryashov, and A. Aleksandrov, *J. Opt. Soc. Am. B* **20**, 1632 (2003).